Simulations of three-dimensional dendritic growth using a coupled thermo-solutal phase-field model

P. C. Bollada, C. E. Goodyer, P. K. Jimack, and A. M. Mullis

Citation: Applied Physics Letters **107**, 053108 (2015); doi: 10.1063/1.4928487
View online: http://dx.doi.org/10.1063/1.4928487
View Table of Contents: http://scitation.aip.org/content/aip/journal/apl/107/5?ver=pdfcov
Published by the AIP Publishing

Simulations of three-dimensional dendritic growth using a coupled thermo-solutal phase-field model

P. C. Bollada,[1,a)] C. E. Goodyer,[2] P. K. Jimack,[1] and A. M. Mullis[3]
[1]*School of Computing, University of Leeds, Leeds LS2 9JT, United Kingdom*
[2]*Numerical Algorithms Group, Oxford OX2 8DR, United Kingdom*
[3]*Institute for Materials Research, University of Leeds, Leeds LS2 9JT, United Kingdom*

(Received 1 June 2015; accepted 31 July 2015; published online 7 August 2015)

Using a phase field model, which fully couples the thermal and solute concentration field, we present simulation results in three dimensions of the rapid dendritic solidification of a class of dilute alloys at the meso scale. The key results are the prediction of steady state tip velocity and radius at varying undercooling and thermal diffusivities. Less computationally demanding 2-dimensional results are directly compared with the corresponding 3-dimensional results, where significant quantitative differences emerge. The simulations provide quantitative predictions for the range of thermal and solutal diffusivities considered and show the effectiveness and potential of the computational techniques employed. These results thus provide benchmark 3-dimensional computations, allow direct comparison with underlying analytical theory, and pave the way for further quantitative results. © *2015 AIP Publishing LLC*. [http://dx.doi.org/10.1063/1.4928487]

There are some problems within science that, due to their complexity, intrinsic interest, and/or practical application, endure for many years or even decades. One such is dendritic growth, this being one of the prime examples in nature of spontaneous pattern formation in a diffusively controlled system. Even the seemingly simple question of making quantitative prediction of the characteristic length scale for a growing dendrite has been proved to be beyond all orders of perturbation theory.[1]

The origins of the problem can be traced back to the pioneering work of Ivantsov,[2] who showed that in the absence of surface energy the shape preserving solution for a solid growing into its undercooled (or supersaturated) parent liquid is a paraboloid of revolution. However, the Ivantsov solution is degenerate in which it relates the product of the growth velocity, V, and the tip radius, ρ, to the undercooling of the parent melt, via the Peclet number, $Pe \equiv \rho V/(2D)$, where D is the diffusivity in the melt. Specifically, the undercooling is related to the Peclet number by the complimentary error function in 2-dimensions and the exponential integral function in 3-dimensions. In contrast, it is always observed experimentally that, for a given physical system, unique values of V and ρ can be associated with given values of the undercooling. Numerous models have subsequently been proposed to break the degeneracy, including growth at the extremum[3] and various models based upon the stability of the growing dendrite,[4] giving rise to theory of growth at marginal stability.[5]

Marginal stability theory makes a number of predictions that have become the "received wisdom" in solidification theory, including that with increasing undercooling the radius of curvature at the tip of an alloy dendrite first passes through a local minimum (as growth moves from solutal control at high solute Peclet number to thermal control at low thermal Peclet number), and then it passes through a local maximum at high thermal Peclet number. However, it has been shown using boundary integral methods that it is the surface energy and specifically the anisotropy in the surface energy that breaks this degeneracy.[6] In fact, the growth of dendrites is not possible in isotropic media, contrary to the predictions of marginal stability theory in which anisotropy is absent. These boundary integral methods have subsequently been developed by a number of authors (e.g., Refs. 1 and 7) into microscopic solvability theory, whereby analytical solutions can be obtained for dendrites growing under the control of a single diffusing species (either heat or solute). In tandem with this has been the development of numerical methods for simulating dendritic morphologies, particularly phase-field methods. Consequently, computational simulation of dendrites under thermal[8] or solute-only control[9] is now a routine, as is the quantitative prediction of characteristic length scales and growth velocities. However, for dendrites growing under coupled thermo-solutal control, as will occur in alloy systems unless the solidification rate is vanishingly small, computational results are sparse.

Quantitative phase-field methods for the coupled thermo-solutal problem have been developed by Ramirez and co-workers,[10,11] but such simulations are computationally challenging due to the multi-scale nature of the problem. Consequently, the simulations presented in Refs. 9 and 12 were restricted to 2-dimensions and for the most part to Lewis number, $Le = 40$. Here, the Lewis number is the ratio of thermal to solutal diffusivity and defines the multi-scale nature of the problem. In contrast, for most metals, which are the most common material to display dendritic solidification, Le is typically around 10 000. By applying a range of advanced numerical techniques, Rosam *et al.*[13] were able to extend the applicability of the model demonstrating that simulations at Le of order 10 000 were feasible[14] in 2-dimensions. However, it is well known that 2-dimensional solidification is quantitatively different from 3-dimensional solidification. Moreover, experimental determination of

a)Email: p.c.bollada@leeds.ac.uk

dendrite growth velocities under coupled thermo-solutal (rapid solidification) conditions is feasible only in bulk (i.e., 3-dimensional) samples. For such bulk samples, a number of containerless processing methods exist for measuring dendrite growth velocities in undercooled metallic alloys, see Refs. 15 and 16, and numerous such datasets exist. For these reasons, we have recently extended the methodology developed in Ref. 12 to 3-dimensions,[17] opening up the feasibility of direct comparison between dendrite growth velocities computed via phase-field simulations with those measured in undercooled liquid metals. Here, we present the first complete data sets for such coupled thermo-solutal simulations of 3-dimensional rapid dendritic growth.

The model we use, along with the computational methods employed, is discussed in detail in Ref. 17. Briefly, non-equilibrium thermodynamic modelling of alloy solidification exploits the quantitative phase field model as developed in Ref. 10, which optimally minimises the total free energy in time whilst conserving solute concentration. Heat flow is modelled by a temperature diffusion equation with a heat source at the solidifying liquid-solid interface. The "thin-interface" formulation[12] is used wherein quantitative valid results, independent of the interface width, are obtained. To give a concise description of the model, we define the dimensionless energy functional

$$F[\phi, U, \theta] = \int_\Omega \left[\frac{1}{2}|A\nabla\phi|^2 + f(\phi) + g(\phi, U, \theta)\right] \mathrm{d}^3x, \quad (1)$$

with a double well potential $f(\phi) \equiv \frac{1}{2}\phi^2 + \frac{1}{4}\phi^4$, bulk forcing term,

$$g(\phi, U, \theta) \equiv \lambda\left(\phi - \frac{2}{3}\phi^3 + \frac{1}{5}\phi^5\right)(\theta + Mc_\infty U) \quad (2)$$

and cubic anisotropy $A \equiv [1 - 3\epsilon + 4\epsilon(n_x^4 + n_y^4 + n_z^4)]$, where $[n_x, n_y, n_z] \equiv \nabla\phi/|\nabla\phi|$. Then the field equations we use, derived in Ref. 10, are given by

$$\tau_\phi \dot{\phi} = -\frac{\delta F}{\delta \phi}, \quad (3)$$

$$\tau_U \dot{U} = \nabla \cdot \left(D_c \frac{1-\phi}{2}\nabla U + \frac{j}{\sqrt{2}}\mathbf{n}\right) + j, \quad (4)$$

$$\dot{\theta} = D_\theta \nabla^2 \theta + \frac{1}{2}\dot{\phi}, \quad (5)$$

with the functions used above are given by

$$j \equiv \frac{1}{2}[1 + (1 - k_E)U]\dot{\phi}, \quad (6)$$

$$\tau_\phi \equiv A^2\left[\frac{1}{Le} + Mc_\infty(1 + (1 - k_E)U\right], \quad (7)$$

$$\tau_U \equiv \left(\frac{1 + k_E}{2} - \frac{1 - k_E}{2}\phi\right). \quad (8)$$

Initial and boundary conditions are given in Ref. 17 as is the efficient evaluation of Eq. (3).

The phase $\phi \in [-1, 1]$ represents bulk liquid at $\phi = -1$ and bulk solid at $\phi = 1$; and thus, the solidification front is defined by the 2-dimensional surface in the 3-dimensional domain where $\phi = 0$. Physical temperature and alloy concentration are recovered, respectively, from

$$\theta = \frac{T - T_M - mc_\infty}{L/C_p}, \quad (9)$$

$$U = \frac{\left(\frac{2c/c_\infty}{1 + k_E - (1 - k_E)\phi}\right) - 1}{1 - k_E}. \quad (10)$$

The material constants introduced in the above are the equilibrium partition coefficient, $k_E \equiv c_S/c_L$ and $Mc_\infty \equiv -mc_\infty(1 - k_E)/(L/C_P)$. The product, Mc_∞, represents the scaled concentration of the starting alloy in the liquid state. In the simulations presented below, we use $Mc_\infty = 0.05$, corresponding to a relatively dilute alloy. As an example, if we were to consider the Ni-Cu system, which displays a single-phase solid solution over the whole composition range and has therefore been the subject of numerous experimental undercooling studies,[16,18] $Mc_\infty = 0.05$ corresponds to $c \sim 17$ wt. % Cu at the Ni-rich end (with $|m| = 2.5\,\mathrm{K/wt.\%}$ at this concentration) or $c \sim 6$ wt. % Ni at the Cu-rich end (with $|m| = 6.0\,\mathrm{K/wt.\%}$ at this concentration).

Table I defines values used in the simulations and Table II gives a glossary of symbols not defined in the text.

In the absence of existing published data on coupled thermo-solutal simulations in 3-dimensions, the following validation regime has been adopted: (i) The code has been reduced to 2-dimensions and the results are validated against published data of Ref. 19; (ii) In Ref. 20, reduced 3-dimensional thermal only results were validated against the model of Karma and Rappel,[21] based upon an explicit implementation described in Ref. 22; (iii) In Ref. 23, reduced 3-dimensional solute only results were validated against the 3-dimensional model developed by Dantzig and co-workers.[24]

As a means of further validation, the phase-field solutions may be compared against the Ivantsov model in the following manner. For known Peclet number, the Ivantsov undercooling, Δ_{Iv}, may be recovered from [see, e.g., Eq. (5) in Ref. 11]: $\Delta_{Iv} = Iv\left(\frac{Pe}{Le}\right) + \frac{Mc_\infty Iv(Pe)}{(1-(1-k_E))Iv(Pe)} + \frac{n(1-15\epsilon)}{\rho}$, where n = 1 in 2D and 2 in 3D. Comparing Δ_{Iv} with the input undercooling to the phase-field simulations, Δ, we find that Δ_{Iv} typically recovers around 85%–101% of Δ, irrespective of whether this is in 2- or 3-dimensions. However, as explained in Ref. 11, care needs to be exercised in selecting the appropriate value of ρ when calculating Pe, with the

TABLE I. Parameter values used for the simulations.

Physical property	Symbol	Value
Anisotropy	ϵ	0.02
Boundary concentration	Mc_∞	0.05
Equilibrium partition coefficient	κ_E	0.3
Dimensionless interface width	λ	2
Solute diffusivity	D	1.2534
Lewis number	Le	40 and 100
Undercooling	Δ	0.25–0.80
Initial nuclear radius	R_0	5.0

TABLE II. Glossary of terms not defined in the text.

Physical property	Symbol
Temperature field	T
Melting temperature	T_M
Solute concentration	c
Solute concentration at boundary	c_∞
Latent heat	L
Heat capacity	C_p
Liquidus gradient	m
Capillary length	d_0
Equilibrium concentration on the solidus (liquidus)	$c_S(c_L)$

parabolic radius of curvature, ρ_{para} (i.e., the radius of curvature of a parabola fitted to the downstream region of the dendrite), being considered more appropriate for this purpose. As ρ_{para} is always larger than ρ, for $\epsilon = 0.02$, typically by 25%–30% (Ref. 25), the higher values of Pe resulting from using ρ_{para} lead to significantly better agreement between Δ and Δ_{Iv}.

Having validated our simulation capability, we now present a comparison of 2D and 3D results for different Lewis numbers and undercooling.

Figures 1 and 2 show the growth velocity, V, and radius of curvature, ρ, at the tip as a function of undercooling, $\Delta = (T - T_M)/(L/C_p)$, for a dendrite growing in 3-dimensions at $Le = 40$ and $Le = 100$. For comparison, the equivalent results for a dendrite growing in 2-dimensions are also shown and data for 2-dimensional growth up to $Le = 500$ are given in Refs. 19 and 26.

We used a mesh size of $\Delta x = 0.39$ on an eighth domain of size 400^3. The discrepancy between $\Delta x = 0.39$ and $\Delta x = 0.195$ is included in the error bars in Figs. 1 and 2 and hence the mesh, $\Delta x = 0.39$, as shown in is sufficiently small. Also included in the error bars for tip radius in Fig. 1 for the 3-dimensional simulations (solid and dotted) is an estimate based upon the final convergence rate. The error was largest for $\Delta = 0.25$, $Le = 40$, for which ρ converged in time very slowly.

The simulations follow, as would be broadly expected from comparison of the analytical solutions for 2- and 3-dimensional growth for a single diffusing species, a more rapid 3-dimensional growth. Similarly, from 2-dimensional simulations, as expected, the 3-dimensional growth velocity also increases with increasing Le. Experimentally

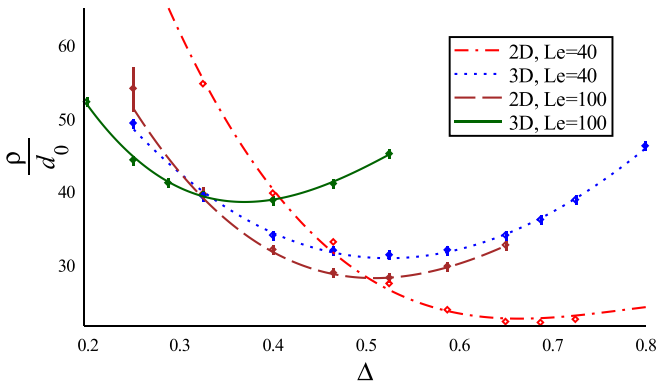

FIG. 1. Relationship between ρ against Δ.

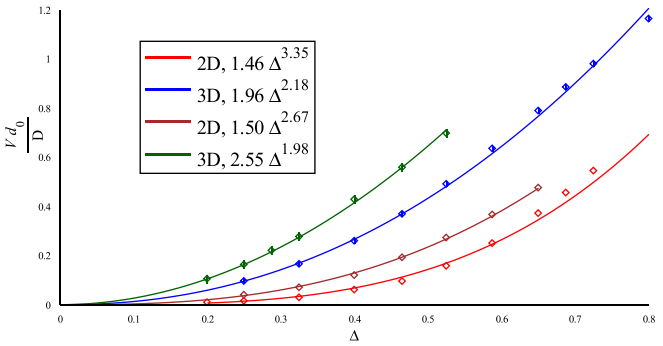

FIG. 2. Relationship between steady state V against Δ.

determined dendrite growth velocities tend to follow a power-law of the form $V \propto \Delta^\beta$, where β is typically in the range of 1.8–4.0, as in these results, but note from Fig. 2, the 3-dimensional cases here exhibit significantly lower values of β than in 2 dimensions.

In 2 dimensions, the tip radius, ρ, displays a minimum with increasing undercooling, a feature which is also observed in the 3-dimensional simulations. With increasing Lewis number, the minimum value of ρ increases while the position of the minimum moves to lower undercooling, a behaviour that is apparent in both the 2- and 3-dimensional datasets. In a similar fashion, if we compare the 2- and 3-dimensional datasets at fixed Lewis number, the minimum value of ρ increases and the position of the minimum moves to lower undercooling. Despite these qualitative similarities in behaviour, the 2- and 3-dimensional data sets are sufficiently different that there does not appear to be any simple way of quantitatively estimating the velocity or tip radius for a dendrite growing in 3 dimensions from a 2-dimensional simulation, necessitating the use of a full 3-dimensional simulation to determine these quantities. In compensation, the 3-dimensional domain is smaller due to the reduced temperature boundary layer. Also, a particular qualitative feature, found in 3-dimensions, is that ρ as a function of time achieves just one maximum before settling to a minimum at steady state, see Ref. 17. This is contrasted at low undercoolings in 2-dimensions ($\Delta < 0.4$, at both Lewis numbers), where ρ exhibits a second maximum appearing much later than the minimum (with consequent substantial 2-dimensional simulation time).

Although both the 2- and 3-dimensional datasets show a minimum with increasing undercooling, neither shows a maximum. This observation has previously been noted with some surprise in relation to the 2-dimensional data[13] given its prediction by marginal stability[5] and its accepted status within solidification theory. The fact that this trend is now seen to be reproduced for 3-dimensional growth, albeit at still rather modest Le, perhaps makes it more likely that the occurrence of a local maximum in ρ with increasing undercooling is not as ubiquitous as suggested by marginal stability theory.

In discussing the breaking of the degeneracy in the solution for dendritic growth and the prediction of the dendrite tip radius, another parameter is often introduced: the stability parameter, $\sigma^* \equiv d_0/(\rho Pe)$. Knowledge of σ^*, together with Pe, which can be calculated analytically, allows the unique

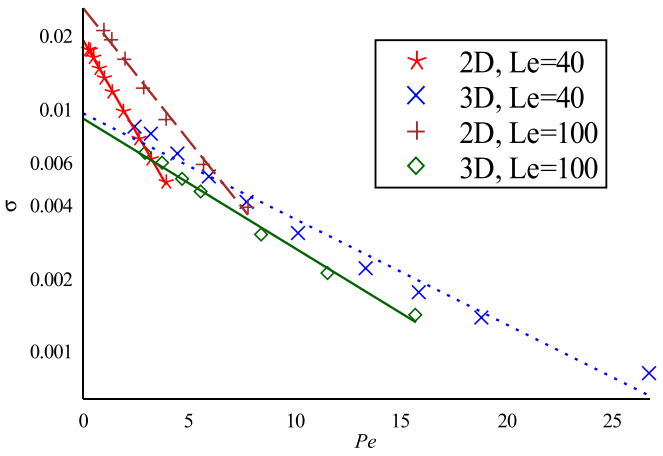

FIG. 3. Approximate exponential trend of σ^* against Pe.

determination of V and ρ. In marginal stability theory,[4,5] σ^* is assumed to be constant wherein, as discussed above, the occurrence of both a local minimum and a local maximum in ρ with increasing undercooling is predicted. In contrast, microscopic solvability theory[1,7] reveals that in the limit of vanishing Peclet number an equation similar to that arising from stability arguments is recovered, but with a radius selection parameter, σ^*, that varies as $\epsilon^{7/4}$. Furthermore, it has also been shown[11,19] that σ^* for alloy systems varies with both undercooling and alloy concentration, c, with the available experimental evidence tending to confirm the latter,[27] and a good agreement with analytical solutions being found in the limits $Le \to \infty$ and $c \to 0$. The variation of σ^* for the simulations reported in this work is shown in Fig. 3, although here we have plotted this as a function of Pe, rather than Δ, wherein an approximate exponentially decreasing trend is revealed.

It is this decrease of σ^* with increasing Pe (or equivalently Δ) that prevents a local maximum in ρ being observed. However, the feature which is most readily apparent from the figure is the very clear distinction between the 2- and 3-dimensional data. This reinforces the view that quantitative 2-dimensional data are likely to be a very poor model for 3-dimensional behaviour and that full 3-dimensional simulations are therefore likely to be needed to obtain quantitative information about dendritic growth in 3-dimensions. However, the variation of σ^* with either Le or Δ appears relatively predictable, meaning that interpolation of results, in any given dimension, between computed undercoolings (or Lewis numbers) may be feasible as it is generally possible to estimate the Peclet number from the undercooling via the exponential integral (or, in 2-dimensions, the complimentary error function). This in turn means that relatively small numbers of computationally intensive simulations may be required, even where large experimental data sets are being fitted.

This research was funded by EPSRC Grant No. EP/H048685. We are also grateful for the use of the HECToR UK National Supercomputing Service.

[1]A. M. Ben and E. A. Brener, Phys. Rev. Lett. **71**, 589 (1993).
[2]G. P. Ivantsov, Dokl. Akad. Nauk SSSR **58**, 567 (1947).
[3]D. E. Temkin, Sov. Phys. Crystallogr. **7**, 354 (1962).
[4]J. S. Langer and H. Muller-Krumbhaar, Acta Metall. **26**, 1681 (1978).
[5]J. Lipton, W. Kurz, and R. Trivedi, Acta Metall. **35**, 957 (1987).
[6]J. S. Langer, *Les Houches, Session XLVI* (Elsevier, New York, 1987).
[7]D. A. Kessler, J. Koplik, and H. Levine, Adv. Phys. **37**, 255 (1988).
[8]A. Wheeler, B. Murray, and R. Schaefer, Physica D **66**, 243 (1993).
[9]J. Warren and W. Boettinger, Acta Metall. Mater. **43**, 689 (1995).
[10]J. C. Ramirez, C. Beckermann, A. Karma, and H. J. Diepers, Phys. Rev. E: Stat., Nonlinear, Soft Matter Phys. **69**, 051607 (2004).
[11]J. C. Ramirez and C. Beckermann, Acta Mater. **53**, 1721 (2005).
[12]A. Karma, Phys. Rev. Lett. **87**, 115701 (2001).
[13]J. Rosam, P. K. Jimack, and A. M. Mullis, J. Comput. Phys. **225**, 1271 (2007).
[14]J. Rosam, P. K. Jimack, and A. M. Mullis, Phys. Rev. E **79**, 030601 (2009).
[15]D. Li, K. Eckler, and D. M. Herlach, Acta Mater. **44**, 2437 (1996).
[16]E. G. Castle, A. M. Mullis, and R. F. Cochrane, Acta Mater. **77**, 76 (2014).
[17]P. C. Bollada, C. E. Goodyer, P. K. Jimack, A. M. Mullis, and F. W. Yang, J. Comput. Phys. **287**, 130 (2015).
[18]E. G. Castle, A. M. Mullis, and R. F. Cochrane, Acta Mater. **66**, 378 (2014).
[19]J. Rosam, P. Jimack, and A. Mullis, Acta Mater. **56**, 4559 (2008).
[20]J. Green, P. K. Jimack, A. M. Mullis, and J. Rosam, Numer. Methods Partial Differ. Equ. **27**, 106 (2011).
[21]A. Karma and W.-J. Rappel, J. Cryst. Growth **174**, 54 (1997).
[22]J. Rosam, "A fully implicit, fully adaptive multigrid method for multiscale phase-field modeling," Ph.D. dissertation (University of Leeds, 2007).
[23]C. E. Goodyer, P. K. Jimack, A. M. Mullis, H. Dong, and Y. Xie, Adv. Appl. Math. Mech. **4**, 665 (2012).
[24]J. H. Jeong, N. Goldenfeld, and J. A. Dantzig, Phys. Rev. E **64**, 041602 (2001).
[25]A. M. Mullis, J. Appl. Phys. **117**, 114305 (2015).
[26]A. M. Mullis, Phys. Rev. E **83**, 061601 (2011).
[27]M. A. Chopra, M. E. Glicksman, and N. B. Singh, Metall. Trans. A **19**, 3087 (1988).